

2026

Peritumoral bone changes in mandibular gingival squamous cell carcinoma: A prospective radiologic-histopathologic correlation study

Gyu-Dong Jo

Kyu-Young Oh

Jo-Eun Kim

Won-Jin Yi

Kyung-Hoe Huh

Follow this and additional works at: <https://jds.ads.org.tw/journal>

Recommended Citation

Jo, Gyu-Dong; Oh, Kyu-Young; Kim, Jo-Eun; Yi, Won-Jin; and Huh, Kyung-Hoe (2026) "Peritumoral bone changes in mandibular gingival squamous cell carcinoma: A prospective radiologic-histopathologic correlation study," *Journal of Dental Sciences*: Vol. 21: Iss. 2, Article 24.

Available at: <https://jds.ads.org.tw/journal/vol21/iss2/24>

This Original Article is brought to you for free and open access by Journal of Dental Sciences. It has been accepted for inclusion in Journal of Dental Sciences by an authorized editor of Journal of Dental Sciences. For more information, please contact cpchiang@ntu.edu.tw.



Available online at <https://jds.ads.org.tw/journal/>

Digital Commons

journal homepage: <https://jds.ads.org.tw/journal/>



Original Article

Peritumoral bone changes in mandibular gingival squamous cell carcinoma: A prospective radiologic-histopathologic correlation study

Gyu-Dong Jo ^{a,c}, Kyu-Young Oh ^{b,c}, Jo-Eun Kim ^c, Won-Jin Yi ^c,
Min-Suk Heo ^c, Sam-Sun Lee ^c, Kyung-Hoe Huh ^{c*}

^a Department of Oral and Maxillofacial Radiology, Yonsei University College of Dentistry, Seoul, Republic of Korea

^b Department of Oral Pathology, College of Dentistry, Dankook University, Cheonan, Republic of Korea

^c Department of Oral and Maxillofacial Radiology, School of Dentistry and Dental Research Institute, Seoul National University, Seoul, Republic of Korea

Received 19 August 2025; Final revision received 25 August 2025

Available online 1 April 2026

KEYWORDS

Squamous cell carcinoma of head and neck;
Mandibular neoplasms;
Magnetic resonance imaging;
Tomography;
X-ray computed;
Neoplasm invasiveness

Abstract *Background/purpose:* Accurate differentiation between tumor invasion and reactive bone response is essential for surgical planning in squamous cell carcinoma (SCC). This prospective study investigated the radiologic-histopathologic correlation of peritumoral bone changes to distinguish malignant invasion from reactive alterations.

Materials and methods: Twenty-four patients with SCC involving the mandibular gingiva or retromolar trigone underwent contrast-enhanced computed tomography (CT) and magnetic resonance imaging (MRI), followed by mandibulectomy. Peritumoral bone was radiologically classified as intact, altered, or infiltrated. Resected specimens underwent cone-beam CT and histopathologic evaluation. Histopathologic classification included: (1) pattern of invasive tumor front (erosive or infiltrative), and (2) type of peritumoral bone change (sclerosis-dominant, fibrosis-dominant, or invasion-dominant). Radiologic and histopathologic findings were correlated, and five-year recurrence and survival rates were analyzed according to histopathologic classifications.

Results: Seventeen of 24 patients exhibited intact or altered peritumoral bone on imaging, which corresponded to sclerosis- or fibrosis-dominant types on histopathology. All infiltrated peritumoral bone cases were histopathologically confirmed as invasion-dominant type, indicating tumor invasion. Patients with sclerosis- or fibrosis-dominant types had significantly

* Corresponding author. Department of Oral and Maxillofacial Radiology, School of Dentistry and Dental Research Institute, Seoul National University, 101 Daehak-ro, Jongno-gu, Seoul 03080, Republic of Korea.

E-mail address: future3@snu.ac.kr (K.-H. Huh).

<https://doi.org/10.1016/j.jds.2025.08.040>

1991-7902/© 2026 Association for Dental Sciences of the Republic of China. Publishing services by Digital Commons. This is an open access article under the CC BY-NC-ND license (<http://creativecommons.org/licenses/by-nc-nd/4.0/>).

better five-year overall survival than those with the invasion-dominant type ($P = 0.04$), although recurrence rates did not significantly differ. Additionally, an infiltrative pattern of invasive tumor front was associated with higher recurrence and mortality compared to an erosive pattern ($P = 0.02$).

Conclusion: Most peritumoral bone changes observed on CT and MRI in mandibular gingival SCC were found to be reactive rather than truly invasive on histopathologic evaluation. Differentiating these changes has prognostic value and helps identify patients with poorer survival.

© 2026 Association for Dental Sciences of the Republic of China. Publishing services by Digital Commons. This is an open access article under the CC BY-NC-ND license (<http://creativecommons.org/licenses/by-nc-nd/4.0/>).

Introduction

Peritumoral tissue (PTT) refers to the non-tumorous tissue immediately surrounding a tumor (typically within 1–3 cm) and is distinct from both healthy and tumor tissues.¹ While historically considered “normal adjacent tissue,” emerging evidence demonstrates that PTT often undergoes significant molecular, histological, and structural changes driven by the tumor.^{2–5} These changes—including inflammation, transcriptional dysregulation, and reactive remodeling—actively contribute to tumor progression and complicate tumor evaluation.

In squamous cell carcinoma (SCC) adjacent to the mandible, the underlying mandibular bone is particularly prone to tumor-related changes. Peritumoral bone can be defined as the mandibular bone marrow space directly beneath the tumor mass, which is most susceptible to SCC-related structural and pathological alterations. Understanding peritumoral bone changes is critical for optimizing surgical margins and treatment planning.^{6,7} Preoperative imaging modalities such as computed tomography (CT) and magnetic resonance imaging (MRI) frequently reveal alterations in peritumoral bone, including trabecular remodeling and abnormal signal intensities.^{8,9} However, these findings do not always indicate malignant invasion, posing challenges in assessing the precise extent of tumor spread. Overestimation of invasion may lead to unnecessarily aggressive resections, compromising postoperative quality of life, whereas underestimation risks insufficient margins, leading to increased recurrence and reduced survival.¹⁰

While peritumoral changes in soft tissues are well-documented, the radiologic-histopathologic correlations of peritumoral bone changes—whether they signify malignant invasion or reactive alteration—remain underexplored, creating a critical gap in understanding SCC progression and prognosis.^{11–20} Addressing this gap is essential for improving diagnostic accuracy and clinical decision-making.

This study prospectively analyzed the radiologic-histopathologic correlation of peritumoral bone changes in mandibular gingival SCC, aiming to differentiate malignant invasion from reactive alteration. These findings are expected to enhance preoperative assessment precision and improve surgical planning and patient outcomes.

Materials and methods

Patients and study design

This prospective study was approved by the Institutional Review Board of Seoul National University Dental Hospital (approval number: IRB007/01–15). Written informed consent was obtained from all participants. Consecutive patients diagnosed with SCC who underwent mandibulectomy at our hospital between October 2016 and December 2017 were included. Eligibility criteria required histopathologically confirmed SCC involving the mandibular gingiva or retromolar trigone, mandibulectomy as the primary surgical intervention, and the availability of comprehensive preoperative CT and MRI, including T1-weighted imaging (T1WI), fat-suppressed T2-weighted imaging (FS-T2WI), and contrast-enhanced fat-suppressed T1-weighted imaging (CE-T1WI) for radiologic assessment. Patients were excluded if they had recurrent SCC, a history of preoperative radiotherapy or chemotherapy, or previous surgical interventions involving the mandible at the SCC site (e.g., tooth extraction or curettage). Additionally, cases with contralateral mandibular marrow alterations that precluded accurate imaging analysis or inadequate specimen size or orientation that prevented reliable radiologic–histopathologic correlation were excluded. Recurrence and survival data were collected through 2024, ensuring a minimum five-year follow-up period.

Radiologic assessment

All patients underwent preoperative CT using a Somatom Sensation 10 scanner (Siemens Healthcare, Erlangen, Germany) with the following parameters: 120 kV tube voltage, 150 mAs tube current, and 1–2 mm section collimation. MRI was performed using either a 1.5-T Signa HDxt system (GE Healthcare, Chicago, IL, USA) or a 3.0-T Skyra system (Siemens Healthcare, Erlangen, Germany). Standard sequences included T1WI, FS-T2WI, and CE-T1WI, with a slice thickness of 4–6 mm and a field of view of 19–22 cm.

Two experienced oral and maxillofacial radiologists (with 7 and 15 years of cancer imaging experience, respectively) independently reviewed all CT and MRI scans.

Table 1 Radiological classification and imaging features of peritumoral bone.

Category	Definition	CT findings	MRI findings
Intact bone	Normal trabecular and marrow structures, with no pathological changes	Normal trabecular attenuation	Normal marrow signal on T1WI and FS-T2WI; no abnormal enhancement on CE-T1WI
Altered bone	Trabecular or marrow abnormalities suspicious for malignancy but lacking definitive invasive features	Increased trabecular attenuation with reduced inter-trabecular space (sclerosis)	Decreased SI on T1WI or increased SI on FS-T2WI or heterogeneous enhancement on CE-T1WI
Infiltrated bone	Complete architectural disruption of trabecular and marrow structures, strongly suggestive of malignant infiltration	Severe trabecular disruption extending variably toward the inferior cortex	Replacement of normal marrow signal by tumor-like SI on T1WI, FS-T2WI, and CE-T1WI

CT, computed tomography; MRI, magnetic resonance imaging; SI, signal intensity; T1WI, T1-weighted imaging; FS-T2WI, fat-suppressed T2-weighted imaging; CE-T1WI, contrast-enhanced fat-suppressed T1-weighted imaging.

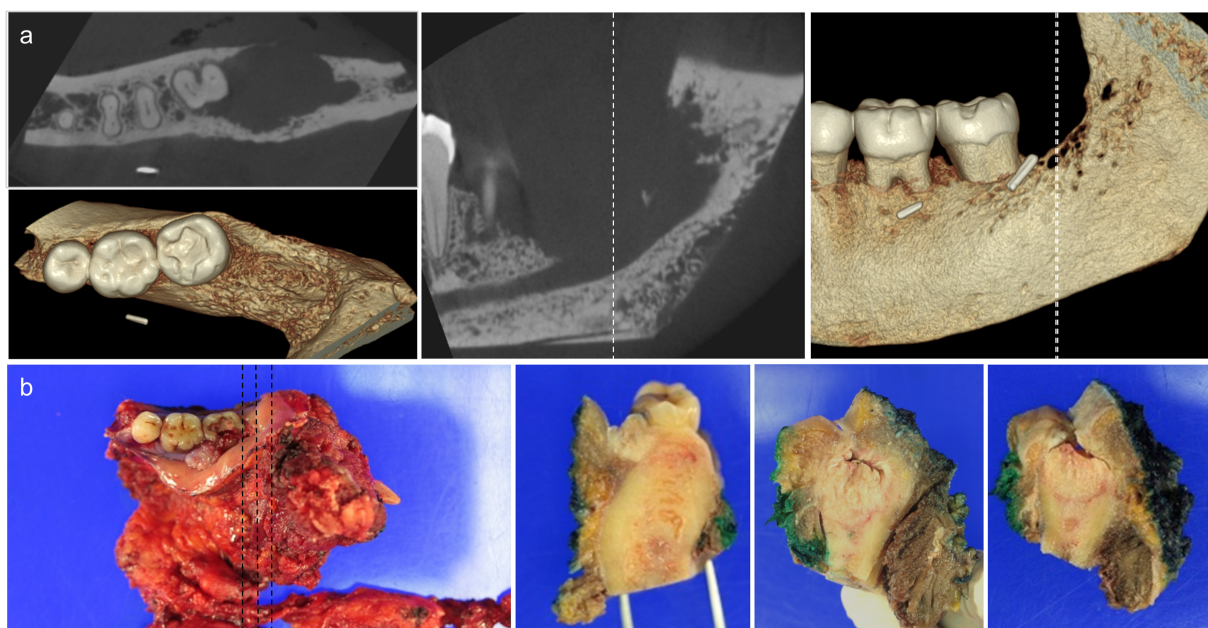


Figure 1 Cone-beam computed tomography (CBCT)-based localization and grossing procedure for histopathologic slide preparation. (A) Post-operative CBCT of the resected specimen illustrating the deepest region of bone destruction (white dashed line). (B) Grossing procedure with 2–3 mm serial sections (black dashed line). Histopathologic slides included the peritumoral bone and adjacent structures.

Table 2 Histopathologic classification of invasive tumor front and peritumoral bone change.

Category	Subtype	Histopathologic features
Type of peritumoral bone change	Sclerosis-dominant type	Sclerotic bone formation leading to loss of trabecular/marrow structure; minimal inflammation; no evidence of tumor invasion
	Fibrosis-dominant type	Fibrosis of the inter-trabecular space resulting in alteration of trabecular/marrow structure; mild to moderate inflammation; no evidence of tumor invasion
	Invasion-dominant type	Tumor infiltration into the inter-trabecular space; severe inflammation; desmoplasia of tumor stroma
Pattern of invasive tumor front	Erosive pattern	Smooth and well-defined tumor-bone interface
	Infiltrative pattern	Irregular and poorly-defined tumor-bone interface

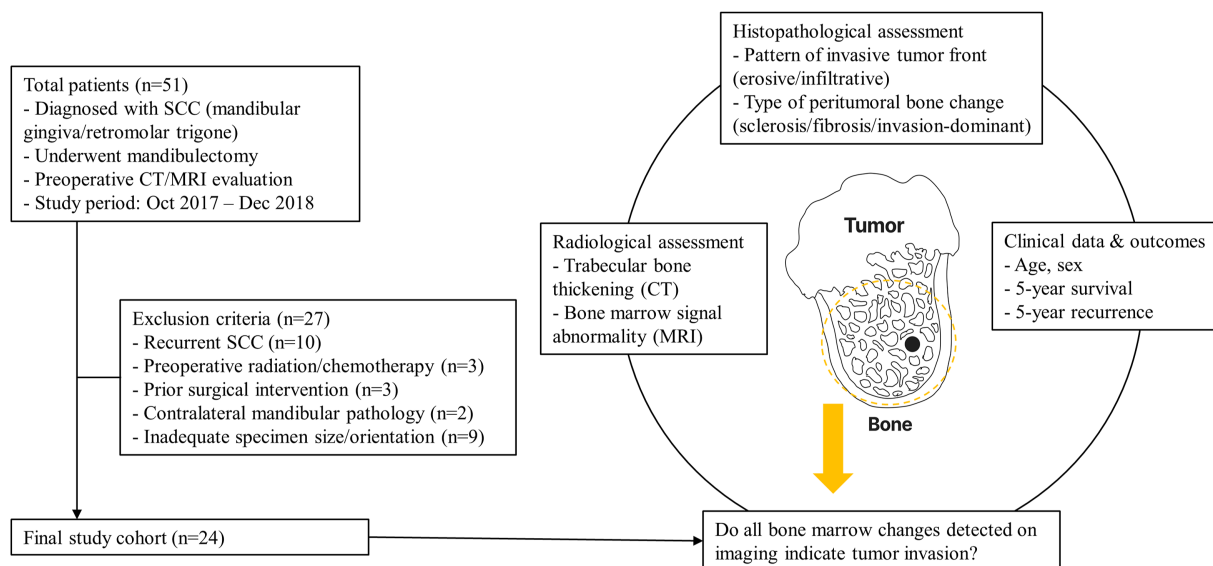


Figure 2 Study cohort selection and analysis framework. Flowchart illustrating the selection of the final study cohort from the initial 51 patients with squamous cell carcinoma. Radiologic, histopathologic, and clinical analyses were conducted to address the key question of whether bone marrow changes on imaging indicate tumor invasion. SCC, squamous cell carcinoma; CT, computed tomography; MRI: magnetic resonance imaging.

Any disagreements in interpretation were resolved by consensus. For each patient, attenuation on CT and signal intensity on MRI were assessed by comparing the involved site to the corresponding contralateral mandibular region.

Peritumoral bone was defined as the segment of mandibular bone marrow space beneath the tumor mass. This region was considered the most susceptible to structural and pathological changes associated with SCC progression. In cases without bone destruction or invasion caused by the tumor mass, evaluation was performed directly below the center of the tumor mass or the area with the greatest tumor thickness. In cases with bone destruction or invasion caused by the tumor mass, evaluation was performed directly below the site of deepest bone destruction.

Based on CT and MRI findings, peritumoral bone changes were classified into three categories: intact bone, altered bone, and infiltrated bone. Table 1 presents the definitions of each category along with characteristic CT and MRI features.

Histopathologic assessment

After mandibulectomy, each surgical specimen was fixed in 10 % neutral-buffered formalin and subsequently scanned using a CS 9300 cone-beam CT system (Carestream, Rochester, NY, USA). CBCT images were reconstructed parallel to the occlusal plane to precisely localize the deepest area of bone destruction identified on preoperative imaging (Fig. 1A). A perpendicular reference line was then drawn from the alveolar crest to the deepest point of tumor-related bone destruction, defining the deepest invasion plane. Based on this reference, the specimen was serially sectioned at 2–3 mm intervals in the anteroposterior direction to ensure accurate correlation with the radiologically defined peritumoral bone (Fig. 1B).

Three histopathologic slides were typically obtained, incorporating the peritumoral bone and adjacent soft tissues.

A single oral pathologist, with over seven years of experience in oral cancer diagnosis, independently evaluated all histologic slides. The pathologist was blinded to the

Table 3 Demographic and clinical characteristics of study cohort.

Characteristics	Value
Total patients	24
Sex	
Male	16
Female	8
Age (years) ^a	64 ± 10 (42–82)
Tumor site	
Mandibular gingiva	16
Retromolar trigone	8
TNM Stage ^b	
I	2
II	4
III	0
IV	18
5-year recurrence	7 (29.2 %)
Mean time to recurrence (months) ^a	18.6 ± 21.3
5-year survival	17 (70.8 %)
Mean survival time among deceased (months) ^a	17.4 ± 12.0

Except where indicated, values represent the number of patients, with percentages in parentheses.

^a Values are mean ± standard deviation, with ranges in parentheses where applicable.

^b TNM staging follows the AJCC 8th edition criteria.

radiologic findings to ensure an unbiased assessment. Two primary histopathologic features were analyzed:

1. Type of peritumoral bone change: A novel classification was introduced to characterize the structural and cellular responses of underlying bone adjacent to SCC. Peritumoral bone changes were categorized into sclerosis-dominant, fibrosis-dominant, and invasion-dominant types, based on the degree of bone remodeling, inflammation, and tumor infiltration.
2. Pattern of invasive tumor front: The tumor-bone interface was classified as either erosive or infiltrative, following established histopathologic criteria.^{21,22}

The detailed classification criteria and histopathologic characteristics are summarized in Table 2.

Clinical data and outcomes

Clinical data and outcomes were obtained by collecting demographic information (age, sex) and five-year recurrence and survival data from electronic medical records and national health insurance databases. These parameters were then analyzed in relation to the histopathologic classifications.

Statistical analysis

The correlation between radiologic and histopathologic findings was assessed using the Chi-square test. The relationship between clinical outcomes and histopathologic findings was analyzed using independent t-tests for continuous variables and Chi-square or Fisher’s exact tests

for categorical variables. Survival analysis was performed using the Kaplan–Meier method, with statistical significance evaluated by the log-rank test. A *P*-value of <0.05 was considered statistically significant. Statistical analyses were conducted using SPSS, version 21.0 (IBM Corp., Armonk, NY, USA).

Results

Patient characteristics

Among 51 patients assessed for eligibility, 24 were included in the final study cohort (Fig. 2). The cohort comprised 16 men and 8 women, with a median age of 63.8 years. The most common tumor site was the mandibular gingiva (67%), followed by the retromolar trigone (33%). During the 5-year follow-up, 7 patients experienced tumor recurrence (mean time to recurrence, 18.6 months), and 7 died (mean survival time among deceased patients, 17.4 months). At the time of final follow-up, 17 patients were alive (Table 3).

Correlation between radiologic and histopathologic findings

Radiologic classifications of peritumoral bone (intact, altered, or infiltrated) on CT, T1WI, FS-T2WI, and CE-T1WI showed a significant association with the histopathologic types (sclerosis-dominant, fibrosis-dominant, and invasion-dominant) (Table 4). Seventeen of the 24 patients exhibited “intact” or “altered” bone changes on imaging, which corresponded to non-invasive, reactive changes upon histopathologic evaluation (i.e., sclerosis- or fibrosis-

Table 4 Correlation between radiological and histopathologic features of peritumoral bone.

	Histopathologic type of peritumoral bone change			<i>P</i>
	Sclerosis-dominant (n = 5)	Fibrosis-dominant (n = 12)	Invasion-dominant (n = 7)	
CT				0.009*
Intact (n = 7)	0	7	0	
Altered (n = 10)	5	5	0	
Infiltrated (n = 7)	0	0	7	
T1WI				0.004*
Intact (n = 8)	1	7	0	
Altered (n = 9)	4	5	0	
Infiltrated (n = 7)	0	0	7	
FS-T2WI				<0.001*
Intact (n = 4)	4	0	0	
Altered (n = 13)	1	12	0	
Infiltrated (n = 7)	0	0	7	
CE-T1WI				<0.001*
Intact (n = 9)	4	5	0	
Altered (n = 8)	1	7	0	
Infiltrated (n = 7)	0	0	7	

* Statistically significant (*P* < 0.05, Chi-square test for trend).

CT, computed tomography; T1WI, T1-weighted image; FS-T2WI, fat-suppressed T2-weighted image; CE-T1WI, contrast-enhanced fat-suppressed T1-weighted image.

dominant, without malignant cell infiltration). Conversely, “infiltrated” findings reliably indicated invasion-dominant changes with confirmed tumor infiltration. These observations suggest that most peritumoral bone changes identified on CT/MRI are reactive rather than truly invasive.

Building on these significant associations, the specific radiological characteristics corresponding to each histopathologic type of the peritumoral bone change are as follows:

1. Sclerosis-dominant type: Characterized by high attenuation on CT and hypointensity on T1WI, reflecting thickened trabecular bone with minimal inflammation (Fig. 3).
2. Fibrosis-dominant type: Demonstrated hyperintense signals on FS-T2WI, consistent with the replacement of fatty marrow by fibrous tissue and varying degrees of inflammation (Fig. 4).
3. Invasion-dominant type: Revealed ill-defined bone destruction on CT and marrow enhancement with indistinct margins on CE-T1WI, corresponding to malignant infiltration and intense inflammation (Fig. 5).

Correlation between clinical and histopathologic findings

Associations between clinical variables (age, sex, recurrence, and survival) and two histopathologic features—type of peritumoral bone change (sclerosis-dominant, fibrosis-dominant, invasion-dominant) and pattern of invasive tumor front (erosive, infiltrative)—were analyzed (Table 5).

The invasion-dominant type of peritumoral bone change was significantly associated with older age, female sex, and increased mortality, but not with recurrence ($P = 0.13$). The infiltrative pattern of invasive tumor front was significantly associated with older age, higher recurrence rates, and increased mortality.

Kaplan–Meier survival analysis demonstrated significantly improved five-year survival in patients with sclerosis-dominant or fibrosis-dominant types of peritumoral bone changes compared with those with invasion-dominant type (Fig. 6A). The survival curves diverged within the first 12 months and remained separated throughout the follow-up period, indicating early and sustained prognostic impact of peritumoral bone changes.

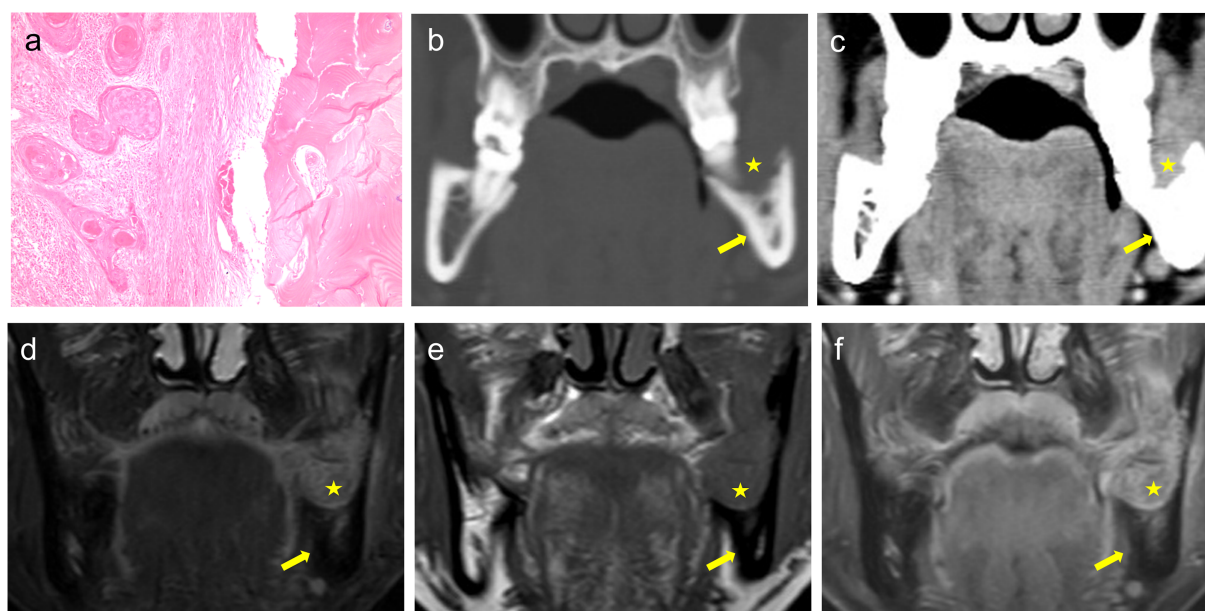


Figure 3 Sclerosis-dominant type.

(A) Histopathologic section from a 57-year-old male patient with oral squamous cell carcinoma. The left side shows the tumor mass with distinct cellular architecture, while the right side exhibits sclerotic bone characterized by obliteration of normal trabecular structure and absence of inflammatory cell infiltration. Hematoxylin and eosin (H&E) stain; original magnification, $\times 100$.

(B) Coronal bone window computed tomography (CT) image of the same patient demonstrates increased bone density, indicative of sclerosis, beneath the tumor mass on the left mandible.

(C) Coronal soft tissue window CT image reveals the tumor mass with irregular margin abutting the sclerotic bone.

(D) Coronal fat-suppressed T2-weighted magnetic resonance (MR) image shows the tumor as a hyperintense lesion, while the sclerotic bone appears hypointense due to its dense mineral content.

(E) Coronal T1-weighted MR image depicts the tumor as isointense signal relative to the muscles, with the adjacent sclerotic bone appearing hypointense signal.

(F) Coronal contrast-enhanced fat-suppressed T1-weighted MR image demonstrates heterogeneous enhancement of the tumor mass, with no significant enhancement observed in the sclerotic bone. Yellow asterisks denote tumor masses, and yellow arrows indicate peritumoral bone changes. (For interpretation of the references to colour in this figure legend, the reader is referred to the Web version of this article).

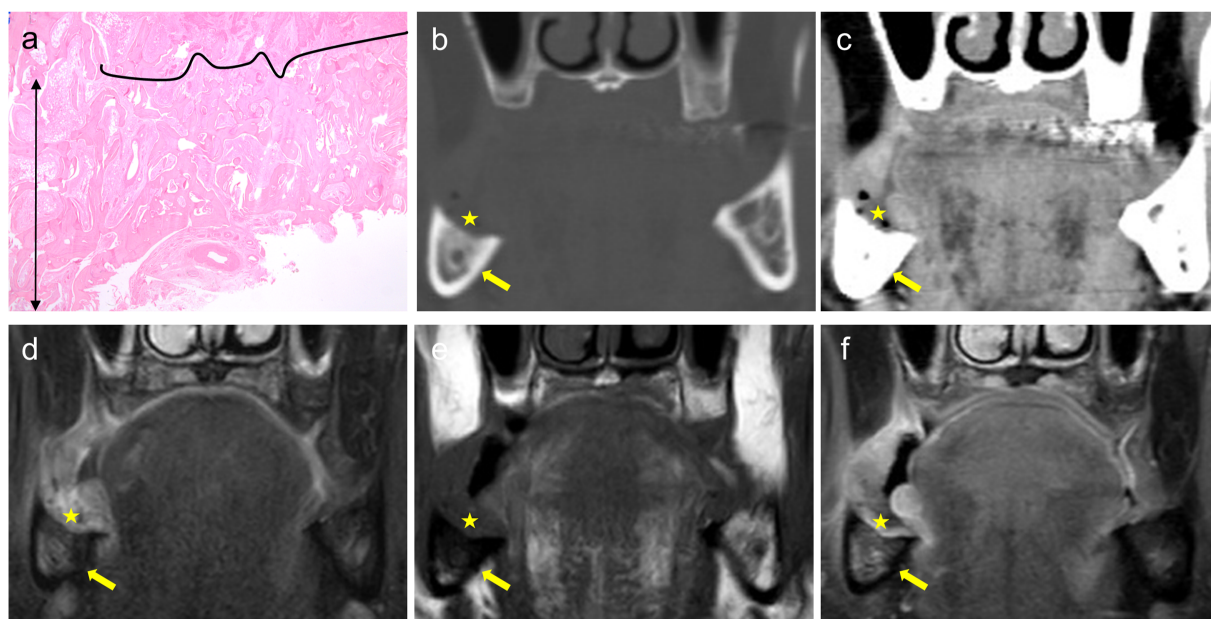


Figure 4 Fibrosis-dominant type.

(A) Histopathologic section from a 58-year-old male patient with oral squamous cell carcinoma. The upper portion of the curved line represents the tumor tissue, while the lower portion delineates a fibrotic zone measuring approximately 0.5 cm in thickness, as indicated by the vertical double-headed arrow. The fibrotic zone demonstrates marked alteration of the normal trabecular structure, extensive fibrosis within the inter-trabecular spaces, and infiltration of inflammatory cells. Hematoxylin and eosin (H&E) stain; original magnification, x12.5.

(B) Coronal bone window computed tomography (CT) image shows trabecular disorganization within the fibrotic zone, adjacent to the tumor mass on the right mandible.

(C) Coronal soft tissue window CT image reveals irregular tumor margins and loss of the clear interface between the tumor mass and surrounding structures.

(D) Coronal fat-suppressed T2-weighted magnetic resonance (MR) image shows a hyperintense fibrotic zone adjacent to the tumor mass.

(E) Coronal T1-weighted MR image demonstrates the fibrotic zone as hypointense signal due to its low water and high collagen content.

(F) Coronal contrast-enhanced fat-suppressed T1-weighted MR image illustrates heterogeneous enhancement of the tumor mass, with minimal enhancement within the fibrotic zone, consistent with its low vascularity. Yellow asterisks denote tumor masses, and yellow arrows indicate peritumoral bone changes. (For interpretation of the references to colour in this figure legend, the reader is referred to the Web version of this article).

Similarly, patients with an erosive pattern of the invasive tumor front exhibited superior survival outcomes compared with those with the infiltrative pattern (Fig. 6B). The erosive group demonstrated 100 % survival throughout the follow-up period, with no recorded deaths, underscoring the excellent prognosis associated with a smooth tumor–bone interface. In contrast, the infiltrative group exhibited an early decline in survival probability, indicating more aggressive tumor behavior associated with poorly defined tumor–bone margins.

Discussion

This prospective radiologic-histopathologic correlation study provides new insight into the nature of peritumoral bone changes in SCC. Contrary to the conventional assumption that radiologic bone alterations on CT and MRI are indicative of malignant invasion, our findings demonstrated that the majority of these changes belonged to the

histopathologically sclerosis-dominant or fibrosis-dominant types, which are interpreted as reactive responses of the bone to tumor presence. Importantly, these types were associated with significantly better five-year survival compared to the invasion-dominant type, although recurrence rates did not differ significantly.

A major strength of this study is the consistent and reproducible association between imaging findings and histopathologic subtypes. Sclerosis-dominant peritumoral bone changes were characterized by increased attenuation on CT and hypointensity on T1WI, while fibrosis-dominant changes exhibited hyperintensity on FS-T2WI. In contrast, invasion-dominant changes displayed marked trabecular destruction on CT and marrow enhancement with indistinct margins on CE-T1WI, suggestive of malignant infiltration. These imaging characteristics may enable radiologists to infer the underlying histopathologic nature of peritumoral bone changes preoperatively.

The prognostic significance of the pattern of invasive tumor front is well established, with the infiltrative pattern

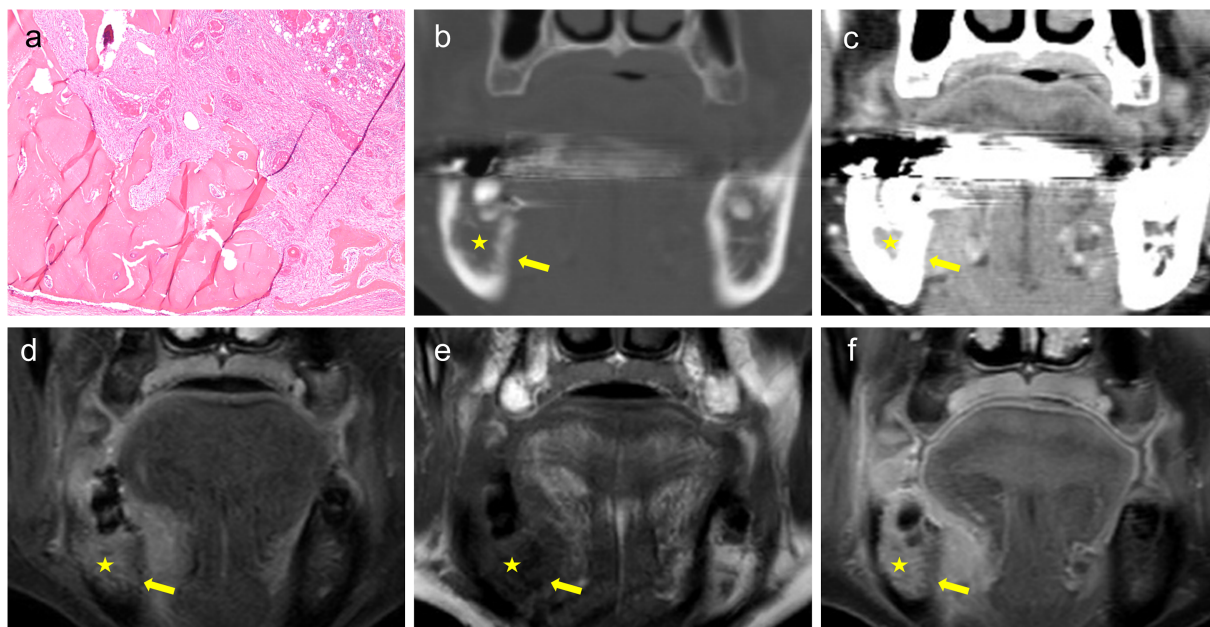


Figure 5 Invasion-dominant type.

(A) Histopathologic section from a 75-year-old female patient with oral squamous cell carcinoma. The image shows malignant tumor islands infiltrating the intertrabecular spaces, accompanied by severe inflammatory cell infiltration. The lower portion of the image includes part of the mandibular inferior cortex, highlighting extensive tumor invasion involving the lower cortical bone. Hematoxylin and eosin (H&E) stain; original magnification, x40.

(B) Coronal bone window computed tomography (CT) image demonstrates destruction of the superior cortex of the right mandible with loss of normal trabecular architecture, consistent with extensive tumor invasion.

(C) Coronal soft tissue window CT image reveals the tumor mass occupying the marrow space.

(D) Coronal fat-suppressed T2-weighted magnetic resonance (MR) image shows a hyperintense tumor mass infiltrating the mandibular bone marrow.

(E) Coronal T1-weighted MR image depicts the tumor as isointense signal relative to the muscles.

(F) Coronal contrast-enhanced fat-suppressed T1-weighted MR image demonstrates heterogeneous enhancement of the tumor mass, with evidence of cortical bone destruction and surrounding soft tissue enhancement.

Yellow asterisks denote tumor masses, and yellow arrows indicate peritumoral bone changes. (For interpretation of the references to colour in this figure legend, the reader is referred to the Web version of this article).

being associated with increased recurrence and mortality.^{23,24} Our findings expand this prognostic framework by demonstrating that the type of peritumoral bone change also correlates with survival outcomes. Specifically, patients with invasion-dominant types showed significantly poorer five-year survival than those with sclerosis- or fibrosis-dominant types. Taken together, these results support a dual-parameter approach—incorporating both the tumor front pattern and the peritumoral bone response type—as a more comprehensive strategy for risk stratification in SCC.

Peritumoral tissue alterations have been extensively investigated in various malignancies, including breast, liver, and brain cancers. In breast cancer, for instance, peritumoral edema and vascular changes on MRI correlate with poor prognosis, while in hepatocellular carcinoma, peritumoral enhancement patterns are predictive of microvascular invasion.^{11–16} In glioblastoma, peritumoral edema on T2-weighted and fluid-attenuated inversion recovery sequences has been shown to reflect tumor-associated inflammation and angiogenesis.^{17–19} These findings highlight the critical role of the tumor microenvironment in shaping both tumor biology and imaging appearance.

In contrast to soft tissue studies, peritumoral bone changes have received little attention.⁸ This study addresses that gap by introducing a structured classification for osseous responses in SCC and correlating these patterns with imaging and clinical outcomes. Our results suggest that sclerosis-dominant and fibrosis-dominant peritumoral bone changes are not incidental but represent host responses to tumor presence, potentially reflecting an interface of stromal remodeling, inflammation, and immune modulation. Recognizing these osseous patterns adds a new dimension to the understanding of the peritumoral microenvironment in SCC and provides a radiologic surrogate for biologic behavior that may inform both prognosis and treatment planning.

Beyond its diagnostic utility, the radiologic–histopathologic correlation demonstrated in this study has practical implications for surgical strategy. For example, a sclerosis-dominant type of peritumoral bone change with an erosive pattern of invasive tumor front may support the consideration of a marginal mandibulectomy, whereas an invasion-dominant type with an infiltrative pattern may indicate the need for a segmental mandibulectomy. Incorporating radiologic criteria into surgical planning has the

Table 5 Correlation between clinical outcomes and histopathologic types/patterns.

	Histopathologic type of peritumoral bone change			<i>P</i>	Histopathologic pattern of invasive tumor front		<i>P</i>
	Non-invasive		Invasive		Erosive (n = 9)	Infiltrative (n = 15)	
	Sclerosis-dominant (n = 5)	Fibrosis-dominant (n = 12)					
Age				0.04 ^a			0.02 ^a
<63.8	3	7	2		6	6	
>63.8	2	5	5		3	9	
Sex				0.02 ^b			0.17 ^b
Male	5	9	2		8	8	
Female	0	3	5		1	7	
Recurrence				0.13 ^b			0.02 ^b
No	5	9	3		9	8	
Recurrence	0	3	4		0	7	
Survival				0.04 ^c			0.02 ^c
Alive	5	9	3		9	8	
Deceased	0	3	4		0	7	

For statistical analysis, sclerosis-dominant and fibrosis-dominant types were grouped as non-invasive and compared with the invasion-dominant (invasive) type.

* Statistically significant ($P < 0.05$).

^a Independent t-test.

^b Fisher's exact test.

^c Kaplan–Meier method with log rank test.

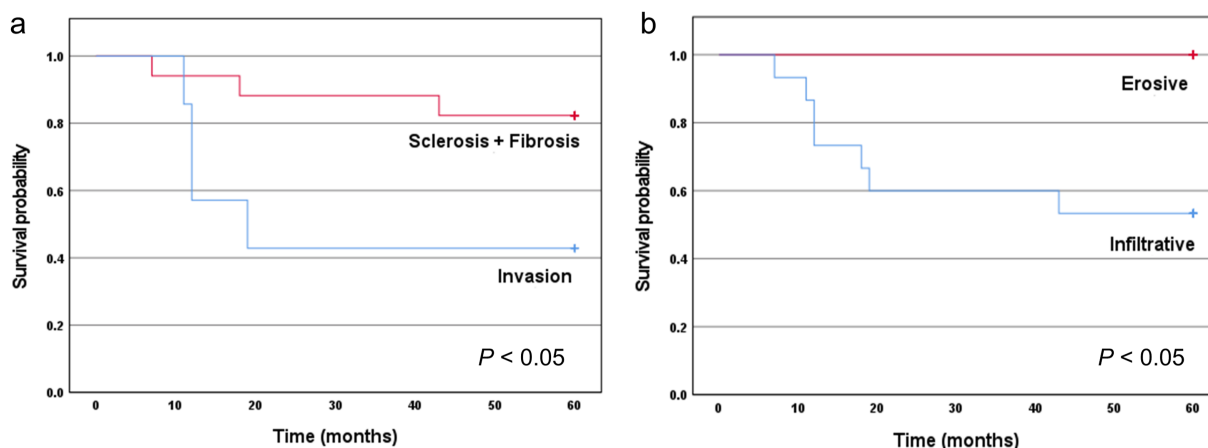


Figure 6 Kaplan–Meier survival curves according to (A) histopathologic type of peritumoral bone change and (B) histopathologic pattern of invasive tumor front.

potential to minimize overtreatment and optimize oncologic outcomes.^{25,26}

This study has several limitations. First, the sample size was relatively small, limiting statistical power and generalizability. Second, the use of 2–3 mm histologic sectioning intervals may have caused false-negative findings, underestimating invasion-dominant types and weakening imaging–pathology correlation. Third, our analysis focused primarily on the vertical extent of bone involvement and did not evaluate horizontal tumor spread or the three-dimensional extent of peritumoral changes. Future studies

involving larger cohorts and advanced image-based quantification techniques are needed to validate and refine the proposed classification system. In addition, further investigation into the molecular and cellular mechanisms underlying sclerosis- and fibrosis-dominant responses in the tumor–bone interface may provide deeper insight into their clinical significance.

In summary, this study demonstrates that most peritumoral bone changes observed on CT and MRI in mandibular gingival SCC represent reactive alterations rather than true invasion. The proposed radiologic–histopathologic

classification enables improved interpretation of imaging findings, supports more individualized surgical planning, and offers prognostic insights.

Declaration of competing interest

The authors have no conflicts of interest relevant to this article.

Acknowledgments

The authors have no acknowledgments.

References

1. Koca D, Abedi-Ardekani B, LeMaout J, Guyon L. Peritumoral tissue (PTT): increasing need for naming convention. *Br J Cancer* 2024;131:1111–5.
2. Qian H, Huang Y, Xu L, Fu H, Lu B. Role of peritumoral tissue analysis in predicting characteristics of hepatocellular carcinoma using ultrasound-based radiomics. *Sci Rep* 2024;14:11538.
3. Ghinda DC, Yang Y, Wu S, et al. Personalized multimodal demarcation of peritumoral tissue in glioma. *JCO Precis Oncol* 2020;4:1128–40.
4. Michot A, Lagarde P, Lesluyes T, et al. Analysis of the peritumoral tissue unveils cellular changes associated with a high risk of recurrence. *Cancers (Basel)* 2023;15:3450.
5. Hayashi Y, Makino T, Sato E, et al. Density and maturity of peritumoral tertiary lymphoid structures in oesophageal squamous cell carcinoma predicts patient survival and response to immune checkpoint inhibitors. *Br J Cancer* 2023;128:2175–85.
6. Russell E, Udkoff J, Knackstedt T. Squamous cell carcinoma with bone invasion: a systematic review and pooled survival analysis. *Dermatol Surg* 2022;48:1025–8.
7. Yoshida S, Shimo T, Muray Y, et al. The prognostic implications of bone invasion in gingival squamous cell carcinoma. *Anti-cancer Res* 2018;38:955–62.
8. Jo GD, Oh KY, Kim JE, et al. Underlying bone change in oral squamous cell carcinoma observed from magnetic resonance imaging and computed tomography: potential implications for tumor aggressiveness and prognosis. *J Dent Sci* 2024;19:2082–9.
9. Jo GD, Yi WJ, Heo MS, Lee SS, Choi SC, Huh KH. CT evaluation of underlying bone sclerosis in patients with oral squamous cell carcinoma: a preliminary retrospective study. *Imaging Sci Dent* 2017;47:255–9.
10. Brandwein-Gensler M, Teixeira MS, Lewis CM, et al. Oral squamous cell carcinoma: histologic risk assessment, but not margin status, is strongly predictive of local disease-free and overall survival. *Am J Surg Pathol* 2005;29:167–78.
11. Park NJ-Y, Jeong JY, Park JY, et al. Peritumoral edema in breast cancer at preoperative MRI: an interpretative study with histopathological review toward understanding tumor micro-environment. *Sci Rep* 2021;11:12992.
12. Zhao S, Li Y, Ning N, et al. Association of peritumoral region features assessed on breast MRI and prognosis of breast cancer: a systematic review and meta-analysis. *Eur Radiol* 2024;34:6108–20.
13. Kadi D, Yamamoto MF, Lerner EC, Jiang H, Fowler KJ, Bashir MR. Imaging prognostication and tumor biology in hepatocellular carcinoma. *J Liver Cancer* 2023;23:284–99.
14. Wu Y, Zhu M, Liu Y, Cao X, Zhang G, Yin L. Peritumoral imaging manifestations on Gd-EOB-DTPA-enhanced MRI for preoperative prediction of microvascular invasion in hepatocellular carcinoma: a systematic review and meta-analysis. *Front Oncol* 2022;12:907076.
15. Yusa T, Yamashita YI, Okabe H, et al. Survival impact of immune cells infiltrating peritumoral area of hepatocellular carcinoma. *Cancer Sci* 2022;113:4048–58.
16. Li H, Liu H, Fu H, et al. Peritumoral tertiary lymphoid structures correlate with protective immunity and improved prognosis in patients with hepatocellular carcinoma. *Front Immunol* 2021;12:648812.
17. Giambra M, Di Cristofori A, Valtorta S, et al. The peritumoral brain zone in glioblastoma: where we are and where we are going. *J Neurosci Res* 2023;101:199–216.
18. Trevisi G, Mangiola A. Current knowledge about the peritumoral microenvironment in glioblastoma. *Cancers* 2023;15:5460.
19. Ballestín A, Armocida D, Ribecco V, Seano G. Peritumoral brain zone in glioblastoma: biological, clinical and mechanical features. *Front Immunol* 2024;15:1347877.
20. Infante JR, Matsubayashi H, Sato N, et al. Peritumoral fibroblast SPARC expression and patient outcome with resectable pancreatic adenocarcinoma. *J Clin Oncol* 2007;25:319–25.
21. Wong RJ, Keel SB, Glynn RJ, Varvares MA. Histological pattern of mandibular invasion by oral squamous cell carcinoma. *Laryngoscope* 2000;110:65–72.
22. Shaw RJ, Brown JS, Woolgar JA, Lowe D, Rogers SN, Vaughan ED. The influence of the pattern of mandibular invasion on recurrence and survival in oral squamous cell carcinoma. *Head Neck* 2004;26:861–9.
23. Kuk SK, Yoon HJ, Hong SD, Hong SP, Lee JI. Staging significance of bone invasion in small-sized (4cm or less) oral squamous cell carcinoma as defined by the American Joint Committee on Cancer. *Oral Oncol* 2016;55:31–6.
24. Ebrahimi A, Murali R, Gao K, Elliott MS, Clark JR. The prognostic and staging implications of bone invasion in oral squamous cell carcinoma. *Cancer* 2011;117:4460–7.
25. Chiesa-Estomba CM, Mayo-Yanez M, Manelli G, et al. Marginal versus segmental mandibulectomy in the treatment of oral cavity cancer: a systematic review and meta-analysis. *Int Arch Otorhinolaryngol* 2023;27:733–43.
26. Gou L, Yang W, Qiao X, et al. Marginal or segmental mandibulectomy: treatment modality selection for oral cancer: a systematic review and meta-analysis. *Int J Oral Maxillofac Surg* 2018;47:1–10.